to the right, its reflection from the surface of the exit channel.

With increasing Reynolds number, the distance between the vortices increases. Figure 5 shows experimental data on the relative distance s/d between the axes of the neighboring vortices as a function of the number Re. This distance was determined from the strips in the central parts of the exit channels of the high cell in the case when colored fluid was supplied to one of the entrance channels. The corresponding values measured in the lower cell lie below them. For Re $\lesssim$ 100 (as measured in the high cell) the flow is steady; above this value, the vortices begin to oscillate. The amplitude of the oscillations is small, and therefore the influence of the unsteady behavior is weakly manifested in the picture of the propagation of the colored strips in the exit channels as captured by the photographs of Fig. 2.

The investigated flow complements the comparatively small number of known flows of a viscous fluid whose instability leads to the formation of regular dynamical structures of a higher order of complexity compared with the structures of the initial flows.

LITERATURE CITED

1. O. Scrivener, C. Berner, R. Cressely, et al., "Dynamical behavior of drag-reducing polymer solutions," J. Non-Newton. Fluid Mech., 5, 475 (1979).
2. A. Keller and J. A. Odell, "The extensibility of macromolecules in solution; a new focus for macromolecular science," Colloid Polymer Sci., 263, 181 (1985).
3. R. S. Farinato, "Elongational flow-induced birefringence of polyacrylamide and poly-(acrylamide-co-sodium acrylate)," Polymer., 29, 2182 (1988).

DEVELOPMENT AND INSTABILITY OF STEADY CONVECTIVE FLOWS IN A SQUARE CAVITY HEATED FROM BELOW AND A FIELD OF VERTICALLY DIRECTED VIBRATIONAL FORCES

A. Yu. Gel'fgat

UDC 532.5.013.4:536.25

The present paper is devoted to numerical investigation of the spatial structure and stability of secondary vibrational convective flows resulting from instability of the equilibrium of a fluid heated from below. Vibrations parallel to the vector of the gravitational force (vertical vibrations) are considered. As in earlier work [7—9], a region of finite size is used — a square cavity heated from below. It is shown that enhancement of the vibrational disturbance of the natural convective flow may either stabilize or destabilize flows with different spatial structures; it may also stabilize certain solutions of the system of convection equations that are unstable in the absence of vibrational forces. In addition, increase of the vibrational Rayleigh number can lead to a change of the mechanisms responsible for equilibrium instability and oscillatory instability of the secondary steady flows.

High-frequency vibrational force fields are effective means of control of thermal vective flows and their stability [1—9]. A well-known example is provided by the oretically predicted [2, 3] and experimentally confirmed [5, 6] possibility of stabi-ing the equilibrium of a fluid heated from below in the case of high-frequency verti-vibrations of a container with fluid. The fluid executes a quasirigid vibrational ion together with the container, and there is no averaged convective flow.

More complicated is the question of the influence of the vibrational forces on teady secondary convective flow that arises after the loss of stability. Secondary ctive flows in a flat horizontal layer were investigated in [4] for different values gravitational and vibrational Rayleigh numbers. Vibrational convective flows in re box were studied in [7—9] in the case when the mutual orientation of the

iga. Translated from Izvestiya Akademii Nauk SSSR, Mekhanika Zhidkosti i Gaza, pp. 9-18, March-April, 1991. Original article submitted February 6, 1990.

0015-4628/91/2602-0165$12.50

© 1991 Plenum Publishing Corporation

vibrational force and the temperature gradient does not allow the existence of convective quasiequilibrium.

In this paper we present an account of the work outlined in the abstract.

The equations that describe the slow (compared with the vibrational component) component of the convective flow have the form [10]

$$\frac{\partial \mathbf{v}}{\partial t}+(\mathbf{v}\nabla)\mathbf{v}=-\nabla p+\Delta \mathbf{v}+[\mathrm{Ra}_g\theta \mathbf{e}_y+\mathrm{Ra}_v(\mathbf{w}\nabla)(\theta\mathbf{n}-\mathbf{w})]\frac{1}{\mathrm{Pr}} \tag{1}$$

$$\frac{\partial \theta}{\partial t}+(\mathbf{v}\nabla)\theta=\frac{\Delta\theta}{\mathrm{Pr}},\quad \mathrm{div}\,\mathbf{v}=0\qquad \mathrm{Ra}_g=\frac{g\beta\Delta\theta l^3}{\nu^2},\quad \mathrm{Ra}_v=\frac{(\beta b\omega\Delta\theta l)^2}{2\nu\chi},\quad \mathrm{Pr}=\frac{\nu}{\chi} \tag{2}$$

where $\mathbf{v}$ is the fluid velocity, θ is the temperature, p is the pressure, Ra_g and Ra_v are the gravitational and vibrational Rayleigh numbers, Pr is the Prandtl number, $\mathbf{e}_y$ is the unit vector in the direction of the y axis, g is the acceleration of free fall, β is the coefficient of volume expansion, $\Delta\theta$ is the difference between the temperatures maintained on the horizontal boundaries of the box, l is its length, ν is its kinematic viscosity, χ is the thermal diffusivity, b and ω are the amplitude and circular frequency of the vibrational motion ($\omega \gg 1$), $\mathbf{n}$ is the unit vector in the direction of the vibration axis, $\mathbf{w}$ is the solenoidal part of the vector $\theta\mathbf{n}$, which on the boundary satisfies the condition $\mathbf{w}\cdot\mathbf{m}=0$, $\mathbf{m}$ is the normal to the boundary.

The boundaries of the box are assumed to be rigid and to conduct heat. On the horizontal boundaries, constant values of the temperature are specified. On the vertical boundaries, a linear distribution $\theta(y)$ is specified:

$$x=0,\ 1;\quad x=1,\quad \mathbf{v}=0,\quad \theta=1-y \tag{3}$$

$$y=0,\ \mathbf{v}=0,\ \theta=1 \tag{4}$$

$$y=1,\ \mathbf{v}=0,\ \theta=0 \tag{5}$$

The validity of the averaged model (1)–(2) has been confirmed experimentally [5–6] and numerically [7]. In particular, for a sufficiently high frequency of the vibrational disturbance, the time-averaged solution of the system of Oberbeck–Boussinesq equations containing the vibrational force and the steady solution of the system (1)–(2) are identical [7].

The problem (1)–(3) resolved by Galerkin's method with coordinate functions constructed by the method proposed in [11]. This method has already been successfully used [12, 13] to investigate the stability of convective flows in a square cavity heated from the side.

The functions $\mathbf{v}$ and θ are approximated by sums

$$\mathbf{v}=\sum_{i=0}^{N}\sum_{j=0}^{N}c_{ij}(t)\varphi_{ij}(x,y),\quad \theta=(1-y)+\sum_{i=0}^{K}\sum_{j=0}^{K}d_{ij}(t)q_{ij}(x,y) \tag{6}$$

The basis functions φ_{ij} and q_{ij} are constructed in the form of linear combinations of Chebyshev polynomials of the first and second kind in such a way as to satisfy all the boundary conditions and the continuity equation (see [11–13]). The function scalar products used in Galerkin's method are defined as follows:

$$(f,g)=\int_V fg\,dV,\quad (\mathbf{u},\mathbf{v})=(u_x,v_x)+(u_y,v_y) \tag{7}$$

The function $\mathbf{w}$ is the solenoidal part of the vector $\theta\mathbf{n}$ and is determined by the system of equations

$$\theta\mathbf{n}=\mathbf{w}+\mathrm{grad}\,\Phi,\quad \mathrm{div}\,\mathbf{w}=0 \tag{8}$$

Setting $w_x=-\partial\Psi/\partial y$ and $w_y=\partial\Psi/\partial x$ and applying the operation curl to the first of Eqs. (8), we obtain

$$\Delta\Psi=-\mathrm{rot}_z(\theta\mathbf{n}) \tag{9}$$

From the condition $\mathbf{w}\cdot\mathbf{m}|_\Gamma=0$ we obtain $\Psi|_\Gamma=0$. Since the boundary conditions for Ψ are identical to those for q_{ij}, Ψ and $\mathbf{w}$ can be approximated by the sums

TABLE 1

Ra_g	Ra_v	Number of vortices	Results of [7, 9]		Our results	
			ψ_{max}	ψ_{min}	ψ_{max}	ψ_{min}
10^4	$4\cdot10^4$	3	5,39	−0.3	5.72	−0,25
10^4	$2{,}5\cdot10^4$	3	5.35	−4.5	5,02	−4,33
0	$4\cdot10^4$	4	1.45	−1.45	1.44	−1,44
0	$4\cdot10^4$	3	2.2	−1.2	2,16	−1,17

$$\psi=\sum_{i=0}^{M}\sum_{j=0}^{M} f_{ij}(t)q_{ij}(x,y),\quad w=\sum_{i=0}^{M}\sum_{j=0}^{M} f_{ij}(t)\varphi_{ij}^{*}(x,y),\quad (\varphi_{ij}^{*})_x=-\partial q_{ij}/\partial y,\quad (\varphi_{ij}^{*})_y=\partial q_{ij}/\partial x \tag{10}$$

It is obvious that on the box boundary $\varphi_{ij}^{*}\cdot\mathbf{m}=0$.

The coefficients f_{ij} can be expressed in terms of the coefficients d_{ij} by solving (9) by Galerkin's method using the expansions (6) and (10). On the other hand, projection of the first of Eqs. (8) onto the φ_{ij}^{*} basis with allowance for the fact that

$$\int_V \varphi_{ij}^{*}\,\mathrm{grad}\,\Phi\,dV=\int_V[\mathrm{div}(\varphi_{ij}^{*}\Phi)-\Phi\,\mathrm{div}\,\varphi_{ij}^{*}]dV=\int_V \Phi\varphi_{ij}^{*}\mathbf{m}\,d\Gamma=0 \tag{11}$$

for any function Φ also gives a relation between f_{ij} and d_{ij}.

By simple manipulations analogous to (11) we can show that

$$(\Delta\psi,\ q_{ij})=-(w,\ \varphi_{ij}^{*}),\quad (\mathrm{rot}_z(0\mathbf{n}),\ q_{ij})=-(0\mathbf{n},\ \varphi_{ij}^{*}) \tag{12}$$

Thus, the two methods of determining the coefficients f_{ij} are equivalent. The explicit expression for the coefficients f_{ij} in terms of the coefficients d_{ij} enables us to avoid the introduction of additional unknown quantities in the computational process, but it does lead to the appearance of additional bilinear terms containing products of the form $c_{ij}d_{k\ell}$ in the equations that determine the coefficients $c_{ij}(t)$. Substitution of (6) and (10) in (1)–(3), calculation of the corresponding scalar products, and expression of the coefficients f_{ij} in terms of the coefficients d_{ij} reduce the problem (1)–(5) to a system of ordinary differential equations of the form

$$\dot{X}_l(t)=a_{lj}X_j(t)+b_{ljk}X_j(t)X_k(t)+F_l \tag{13}$$

where $X_\ell(t)$ is one of the coefficients $c_{ij}(t)$ or $d_{ij}(t)$.

Steady solutions of the system of equations (13) corresponding to steady solutions of the problem (1)–(5) were determined in [12, 13] by Newton's method. In the case of heating from below, the problem (1)–(5) has different forms of spatial symmetry, and therefore Newton's method makes it possible to obtain solutions that possess the same type of symmetry as the initial approximation, which must be chosen sufficiently far from the trivial solution $X_\ell = 0$. Therefore, in the cases when it is necessary to find a steady solution with a previously unknown spatial structure the stabilization method was used, i.e., continuation of the iteration procedure until the solution stabilizes. The stability of the steady solutions was investigated in the same way as in [12, 13].

In the case when a Hopf bifurcation is discovered, it is assumed that the frequency of the vibrational motion is much higher than the frequency of the oscillatory flow that appears. In the case of the occurrence of one zero eigenvalue (monotonic instability), the flow in the supercritical region was determined by the stabilization method. In the cases when integration of the system of equations (13) with respect to the time led to a new steady solution, the stability of this solution was also investigated. Despite the monotonic instability, in some cases integration with respect to the time led to the appearance of an oscillating solution, indicating the presence of an oscillatory instability that develops in a manner different from Hopf bifurcation.

The results of [7, 9] relating to vibrational–gravitational convection of a fluid Pr = 1 in a square box heated from the side ($F_\ell \neq 0$) were used to test the viability

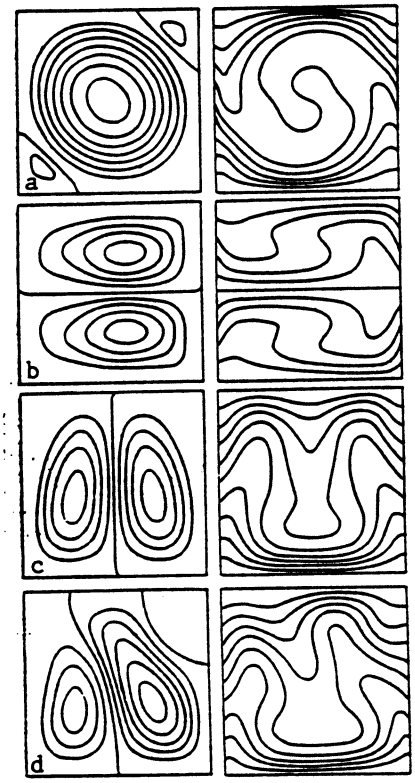

Fig. 1

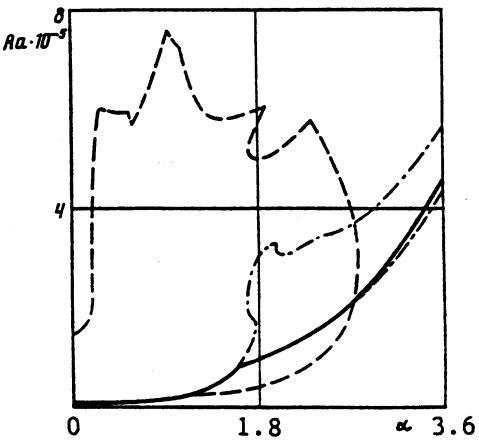

Fig. 2

of the employed numerical method. The extremal values of the flow function obtained for different values of Ra_g and Ra_v in [7, 9] and in the present work for N = M = K = 6 agree well (see Table 1). Bifurcation from the 4-vortex to the 3-vortex flow regime in the case $Ra_g = 0$ occurs at $Ra_v > 1.5 \cdot 10^4$ [9]. In the present work, the obtained value of Ra_v corresponding to this bifurcation is $Ra_v^* = 1.88 \cdot 10^4$.

Calculations were made for three fixed values of the Prandtl number: 0.02, 1, 15. The streamlines and isotherms of the steady convective flows corresponding to different forms of spatial symmetry are shown in Fig. 1. For the three values of the Prandtl number we obtained in the plane of Ra_g and $\alpha = Ra_v/Ra_g$ regions of flow stability possessing central symmetry with respect to the center of the box (Fig. 1a, $Ra_g = 1.4 \cdot 10^5$, $Ra_v = 0$, Pr = 0.02, $|\psi|_{max} = 1420$), reflection symmetry about the line x = 0.5 (Fig. 1b, $Ra_g = 2.2 \cdot 10^5$, $Ra_v = 6.6 \cdot 10^5$, Pr = 1, $|\psi|_{max} = 11.1$), and reflection symmetry about the line y = 0.5 (Fig. 1c, $Ra_g = 4.5 \cdot 10^4$, $Ra_v = 0$, Pr = 15, $|\psi|_{max} = 0.523$); ψ is the flow function. An example of asymmetric convective flow that is the outcome of instability of the symmetric flow in Fig. 1c is shown in Fig. 1b ($Ra_g = 6 \cdot 10^4$, $Ra_v = 0$, Pr = 15, $\psi_{max} = 0.52$, $\psi_{min} = -0.61$). The results of the stability investigation are shown for Pr = 0.02, 1, and 15 in Figs. 2–4, respectively.

The continuous curves in Figs. 2–4 correspond to equilibrium instability. The broken curves bound the regions of stability of flows that are centrally symmetric with respect to the center of the box (see Fig. 1a). The chain curves correspond to the stability boundaries of the flows that are reflection symmetric with respect to the line y = 0.5 (see Fig. 1b, curves 1 in Figs. 2–4) and the asymmetric flows that develop from them (see Fig. 1c, curves 2 in Figs. 2–4). The broken curves 3, 4, 6 in Fig. 4 (Pr = 15) shows the stability region of the flows that are reflection symmetric with respect to the line x = 0.5 (Fig. 1c), while curves 4 and 5 bound the stability region of the corresponding asymmetric flows (see Fig. 1d). Such flows become stable for sufficiently large Prandtl numbers. With decreasing Pr, the region bounded by curves 3, 5, 6 and the ordinate gradually contracts and then disappears. In Fig. 3, for Pr = 1, this region is shown schematically by the broken curves. For Pr = 0.02, the flows with the spatial structure shown in Figs. 1c and 1d are unstable for all values of Ra_g and Ra_v.

The neutral curves corresponding to equilibrium instability (the continuous curves

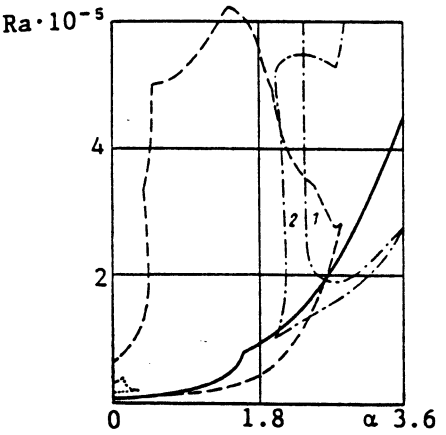

Fig. 3

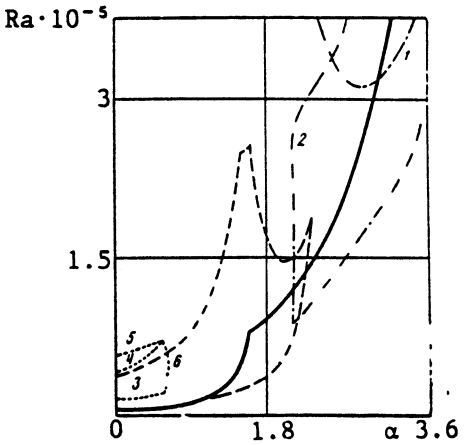

Fig. 4

in Figs. 2—4) have a break at $\alpha = 1.6$, the position of which does not depend on the Prandtl number.

For $\alpha < 1.6$, the most dangerous disturbance of the convective quasiequilibrium possesses central symmetry, and a centrally symmetric flow arises as a result of the instability (see Fig. 1a). For $\alpha > 1.6$, the perturbation possessing reflection symmetry about the line $y = 0.5$ becomes the most dangerous. The secondary convective flow corresponding to this disturbance (see Fig. 1b) is stable in the case of small Prandtl numbers when $\alpha > 1.6$ (chain curve in Fig. 2). However, at higher Prandtl numbers such flows become stable only for $\alpha > 2$, and it is the corresponding asymmetric flows (curves 2 in Figs. 3—4) that first become stable, only then being followed by the symmetric flows (curves 1 in Fig. 3—4). As can be seen from Figs. 2—4, enhancement of the vibrational disturbance leads to the appearance of hysteresis phenomena — the steady flows may remain stable in the region that is subcritical from the point of view of equilibrium stability.

The results relating to oscillatory instability have physical meaning only in the cases when the frequency ω_0 of the oscillatory convective flow that develops after the loss of stability is much lower than the frequency ω of the vibrational motion: $\omega \gg \omega_0$. If the transition to the oscillatory regime takes place through a Hopf bifurcation, then the imaginary part of the dominant eigenvalue will serve as an estimate of ω_0. The maximal dimensionless values of ω_0 (the dimensional scale is χ/ℓ^2) obtained in the process of the stability investigation can be estimated as follows: for the centrally symmetric flows (Fig. 1a) $\omega_0 = 2 \cdot 10^3$; for the flows consisting of two vertically situated vortices (Figs. 1c and 1d), $\omega_0 = 600$; for flows consisting of two vortices with one above the other, $\omega_0 = 450$. As a rule, the dimensional frequency scale χ/ℓ^2 is less than 10^{-4} Hz, and therefore the obtained values of ω_0 correspond to oscillations with frequency that do not exceed 1 Hz, this fully corresponding to the considered averaged model.

The physical mechanisms giving rise to instability of the steady convective flows are characterized at critical values of the parameters by the eigenvector of the problem (1)—(4) linearized in the neighborhood of the steady flow that corresponds to the dominant eigenvalue. Since the components of the eigenvector are complex numbers, a certain physical meaning corresponds to the modulus of the most dangerous perturbation, the value of which in the case of Hopf bifurcation characterizes the spatial distribution of the rms amplitude of the pulsations that grow exponentially at the time when stability is lost. The breaks in the neutral curves shown in Figs. 2—4 correspond to replacement of the one most dangerous disturbance by the other. Analysis of the spatial structure of the most dangerous infinitesimally small disturbance makes it possible to study the supercritical mechanisms responsible for the instability of the convective flow.

In Figs. 5—7, the continuous curves show the streamlines (on the left) and isotherms (on the right) of the steady convective flows that are losing stability, while the broken curves are the isolines of the absolute value of the most dangerous infinitesimally small disturbance of the flow function and temperature. The development of the oscillatory instability can be represented as a sum of the time-constant flows shown in Figs. 5—7 by the continuous curves and the pulsating terms with exponentially growing amplitude

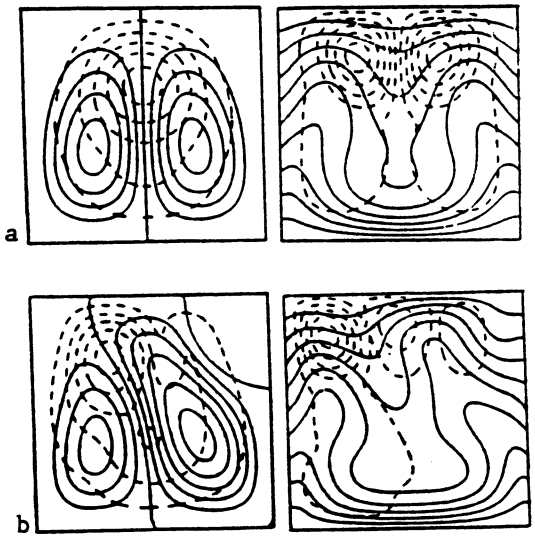

Fig. 5

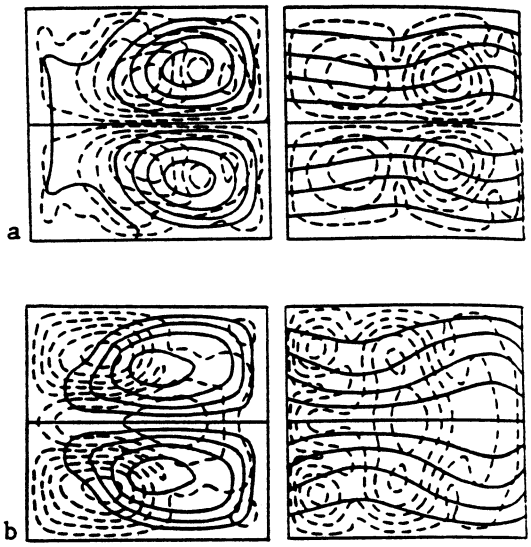

Fig. 6

(broken curves in Figs. 5–7).

Figure 5 shows the convective flows and the most dangerous disturbances of them for symmetric and asymmetric flows consisting of two convective vortices (see Figs. 1c and 1d). The flows symmetric with respect to the line x = 0.5 become stable above curve 3 (see Fig. 4). With increasing Ra_g these flows become unstable (curve 4) and bifurcate to a steady asymmetric flow. With further increase of Ra_g above curve 5 the asymmetric flow becomes unstable with respect to oscillatory disturbances. On the other hand, with increasing α to the right of curve 6 it is the symmetric flow that acquires oscillatory instability. Figure 5a corresponds to the oscillatory instability of the symmetric flow that arises on curve 6 ($Ra_g = 3.75 \cdot 10^4$, $\alpha = 0.6$, Pr = 15) and Fig. 5b corresponds to the one on curve 5 ($Ra_g = 6 \cdot 10^4$, $\alpha = 0$, Pr = 15). In both cases, the spatial structures of the most dangerous disturbances are similar and differ only in the presence or absence of symmetry. The maximal value of the disturbance of the flow function is on the boundary that separates the two convective vortices, while the maximal value of the temperature disturbance occurs on both sides of the line separating the vortices in the upper part of the region, where the flow has a comparatively low intensity. This suggests that in the given case the oscillatory instability arises on the boundary separating the two convective vortices, in the region of comparatively slow flow. Integration of the system (15) with respect to the time shows that in the case represented in Fig. 5a the oscillatory instability leads to loss of reflection symmetry and that the convective oscillations are pulsations of two vortices whose intensities vary in antiphase.

Figure 6 illustrates the loss of stability by steady convective flows consisting of two vortices with one above the other. Such flows become stable at sufficiently large values of α. Oscillatory instability of the flow with reflection symmetry with respect to the line y = 0.5 was observed only for Pr = 0.02 (chain curve in Fig. 2). The different spatial structures of the most dangerous disturbance for this case are shown in Figs. 6a–6c. In the case shown in Fig. 6a ($Ra_g = 2.8 \cdot 10^5$, $\alpha = 1.8$) the most intense disturbances of the flow are near the extremal values of the flow function. At the same time, the oscillatory mode that generates the instability either destroys the existing convective vortices or gives rise to oscillations of two reflection-symmetric vortices. At large α (see Fig. 6b, $Ra_g = 4 \cdot 10^5$, $\alpha = 3$) the strongest disturbances are observed in the region of comparatively slow convective flow and on the boundary separating the two convective vortices. In this case the development of the oscillatory instability leads to a qualitative rearrangement of the spatial structure of the flow, in particular to a loss of reflection symmetry.

For Pr = 1 and 15, the flows with reflection symmetry about the line y = 0.5 lose stability with respect to monotonic disturbances to the left and below curves 1 in Fig. 3–4. The instability results in the development of asymmetric flows consisting of two convective vortices with one above the other. The oscillatory instability of the

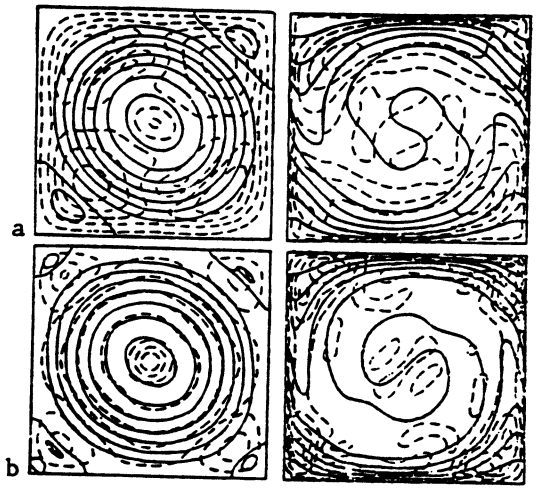

Fig. 7

asymmetric flows occurs above curves 2 in Fig. 3 and 4. The stability is lost in the same way as in the case shown in Fig. 6a, but in the case of asymmetric flow only the one most intense convective vortex becomes unstable.

The greatest diversity of different spatial structures of the most dangerous infinitesimally small disturbance is observed in the stability analysis of the centrally symmetric flows. However, they are all different combinations of the three instability mechanisms illustrated in Figs. 7a and 7b.

Figure 7a ($Ra_g = 1.4 \cdot 10^5$, $\alpha = 0$) illustrates loss of stability with rapid increase of the thermal and hydrodynamic disturbances at the box boundaries; this characterizes the instability of a closed boundary layer. The most intense disturbances of the flow function and the temperature are on the diagonals of the square and are displaced from the center toward the box corners. In the central part of the flow, the disturbances have a relatively weak intensity.

Figure 7b ($Ra_g = 5.4 \cdot 10^5$, $\alpha = 1$) shows the case when the global maximum of the absolute value of the disturbance of the flow function is at the center of the cavity, while lesser maxima are situated on the diagonals between the main and reverse convective vortices. The maxima of the absolute value of the temperature disturbance are also near the reverse vortices, whereas in the center of the box the temperature disturbance is comparatively small. In the considered case, one can clearly see the two characteristic reasons for the oscillatory instability: the instability of the main convective vortex and the instability due to the interaction of the main and reverse convective vortices.

The most dangerous infinitesimally small disturbances of centrally symmetric convective flows can also have other spatial structures very different from those shown in Fig. 7. However, in all cases the isolines of the absolute value of the disturbances indicate the presence of different combinations of these two instability mechanisms.

The transition from the steady to the oscillatory solution does not always occur through a Hopf bifurcation. In some cases, nonsteady calculations for supercritical values of the parameters make it possible to establish that the instability determined by zero eigenvalue of the Jacobi matrix is oscillatory. In particular, such instability is observed in the case of intersection of the curves 1 (see Figs. 3 and 4) from the right to the left above the point of intersection of these curves with curves 2. The oscillatory instability of the centrally symmetric flows for $Pr \geq 1$ and comparatively small α also sets in in this manner (left-hand smooth section of the broken curve in Figs. 3 and 4). Thus, the nonsteady calculation made for $Pr = 1$, $Ra_v = 0$, $Ra_g = 7 \cdot 10^4$ using the centrally symmetric flow as initial condition made it possible to discover an oscillatory regime with several multiple frequencies. The time and spatial characteristics of the obtained oscillatory solution correspond to the results obtained in [14] for $Ra_g = 7 \cdot 10^4$ and $Pr = 0.71$. At the same time, the solution of the nonstationary convection equations, averaged over a period of the oscillations, is reflection symmetric about the line $y = 0.5$, i.e., in this case the monotonic instability gives rise to a transition from a centrally symmetric to a reflection-symmetric steady flow, which, in

its turn, is unstable with respect to oscillatory disturbances.

Thus, high-frequency vertically directed vibrational forces have a quite different effect on steady convective flows with different spatial structures. Relatively weak vibration fields have a strong stabilizing effect on centrally symmetric convective flow but an increase of the vibrational Rayleigh number may lead to a lowering of the stability threshold of such flows, this even going so far as complete destabilization of them (broken curves in Figs. 2–4).

Similarly, gradual increase of Ra_v from zero to Ra_v^* stabilizes flows that are reflection symmetric about the line $x = 0.5$. For $Ra_v > Ra_v^*$, these flows are completely destabilized (broken curves in Figs. 3 and 4).

The considered vibrational forces have an essentially new effect on flows that are reflection symmetric with respect to the horizontal plane (chain curves in Figs. 2–4). These flows become stable when α reaches a definite threshold value (break in the neutral stability curves of convective equilibrium at $\alpha = 1.6$, Figs. 2–4) and they become unstable when the parameter α of the vibrational disturbance decreases rather than increa

I thank G. Z. Gershuni for assistance and extremely fruitful discussions of the results of the paper.

LITERATURE CITED

1. G. Z. Gershuni, N. M. Zhukhovitskii, and A. A. Nepomnyashchii, Stability of Convec Flows [in Russian], Nauka, Moscow (1989).
2. G. Z. Gershuni and E. M. Zhukhovitskii, Convective Stability of an Incompressible Fluid [in Russian], Nauka, Moscow (1972).
3. S. M. Zen'kovskaya I. B. Simonenko, "Influence of high-frequency vibrations on th onset of convection," Izv. Akad. Nauk SSSR, Mekh. Zhidk. Gaza, No. 5, 51 (1966).
4. S. M. Zen'kovskaya and S. N. Ovchinnikova, "Calculation of secondary flows in a p lem of thermovibrational convection in a layer," Rostov-on-Don (1987) (Paper Depo at VINITI on June 24, 1987, No. 4579-V87).
5. M. P. Zavarykin, S. V. Zorin, and G. F. Putin, "Experimental investigation of vi tional convection," Dokl. Akad. Nauk SSSR, 281, 815 (1985).
6. M. P. Zavarykin, S. V. Zorin, and G. F. Putin, "Thermoconvective instability in vibration field," Dokl. Akad. Nauk SSSR, 299, 309 (1988).
7. G. Z. Gershuni, E. M. Shukhovitskii, and Yu. S. Yurkov, "Numerical investigation of free convection in a closed cavity executing vertical vibrations," in: Numer Methods of the Dynamics of Viscous Fluids [in Russian], Novosibirsk (1979), p.
8. G. Z. Gershuni, E. M. Zhukhovitskii, and Yu. S. Yurkov, "Convective oscillation in a closed cavity in a modulated gravity field," in: Convective Flows, No. 1 [Russian], Perm' (1979), p. 73.
9. G. Z. Gershuni, E. M. Zhukhovitskii, and Yu. S. Yurkov, "Vibrational thermal co tion in a rectangular cavity," Izv. Akad. Nauk SSSR, Mekh. Zhidk. Gaza, No. 4, (1982).
10. I. B. Simonenko, "Justification of the method of averaging for a problem of co tion in a field of rapidly oscillating forces and for other parabolic equation Mat. Sb., 87, 236 (1972).
11. A. Yu. Gel'fgat, "Variational method of solution of problems in the dynamics of fluid in rectangular regions," in: Applied Problems of Mathematics and Physics Russian], Riga (1987), p. 14.
12. A. Yu. Gel'fgat and B. Ya. Martuzan, "Stability and oscillatory regimes of na convection in a rectangular box heated from the side," in: Applied Problems o ematics and Physics [in Russian], Riga (1988), p. 31.
13. A. Yu. Gel'fgat, "Influence of the magnitude and direction of a magnetic fie the oscillatory regimes of thermogravitational convection in a rectangular c Magn. Gidrodin., No. 3, 70 (1988).
14. I. Goldhirsch, R. B. Pelz, and S. A. Orszag, "Numerical simulation of therma tion in a two-dimensional finite box," J. Fluid Mech., 199, 1 (1989).